www.czasopisma.pan.pl PAN POLSKA AKADEMIA NAUK www.journals.pan.pl

ARCHIVES OF ACOUSTICS
Vol. **44**, No. 4, pp. 637–644 (2019)
DOI: 10.24425/aoa.2019.129276

Assessment of High Frequency Imaging and Doppler System for the Measurements of the Radial Artery Flow-Mediated Dilation

Andrzej NOWICKI[(1)]*, Barbara GAMBIN[(1)], Wojciech SECOMSKI[(1)], Zbigniew TRAWINSKI[(1)]
Michał SZUBIELSKI[(2)], Ryszard TYMKIEWICZ[(1)], Robert OLSZEWSKI[(1),(3)]

[(1)] *Institute of the Fundamental Technological Research*
Polish Academy of Sciences
Pawinskiego 5B, 02-106 Warsaw, Poland
*Corresponding Author e-mail: anowicki@ippt.gov.pl

[(2)] *Mazovia Regional Hospital in Siedlce*
Siedlce, Poland

[(3)] *Department of Gerontology, Public Health and Didactics*
National Institute of Geriatrics, Rheumatology and Rehabilitation
Warsaw, Poland

(*received May 28, 2019; accepted June 27, 2019*)

Objectives: In the article we describe the new, high frequency, 20 MHz scanning/Doppler probe designed to measure the flow mediated dilation (FMD) and shear rate (SR) close to the radial artery wall.

Methods: We compare two US scanning systems, standard vascular modality working below 12 MHz and high frequency 20 MHz system designed for FMD and SR measurements. Axial resolutions of both systems were compared by imaging of two closely spaced food plastic foils immersed in water and by measuring systolic/diastolic diameter changes in the radial artery. The sensitivities of Doppler modalities were also determined. The diagnostic potential of a high frequency system in measurements of FMD and SR was studied *in vivo*, in two groups of subjects, 12 healthy volunteers and 14 patients with stable coronary artery disease (CAD).

Results: Over three times better axial resolution was demonstrated for a high frequency system. Also, the sensitivity of the external single transducer 20 MHz pulse Doppler proved to be over 20 dB better (in terms of a signal-to-noise ratio) than the pulse Doppler incorporated into the linear array. Statistically significant differences in FMD and FMD/SR values for healthy volunteers and CAD patients were confirmed, p-values < 0.05. The areas under Receiver Operating Characteristic (ROC) curves for FMD and FMD/SR for the prediction CAD had the values of 0.99 and 0.97, respectively.

Conclusions: These results justify the usefulness of the designed high-frequency scanning system to determine the FMD and SR in the radial artery as predictors of coronary arterial disease.

Keywords: flow mediated dilation; shear rate; axial resolution; elevation resolution; pulsed Doppler; ultrasonic imaging.

1. Introduction

The process of development of atherosclerotic diseases is preceded by endothelial dysfunction of blood vessels, decreased bioavailability of nitric oxide (NO) and the development of a local inflammatory process (Yousuf *et al.*, 2013; Koeth *et al.*, 2013). Dysfunction of vascular endothelium leads to cardiovascular disease (Lehoux *et al.*, 2016; Cahill *et al.*, 2016; Deshko *et al.*, 2011; Deanfield *et al.*, 2007; Gutiérrez *et al.*, 2013). Celermajer *et al.* (1992) introduced the method of ultrasonographic recording of the brachial artery diameter changes induced, within several minutes, by reactive arm hyperaemia. It was demonstrated that a change of the magnitude of FMD also depends on the value of the shear rate stimulus

(Pyke *et al.*, 2004; 2007; Padilla *et al.*, 2008; Harris *et al.*, 2010). In the recently published review article (Storch *et al.*, 2017), ultrasound measurements of (FMD) were classified as a promising tool to assess endothelial function, however with some limitations. Among the limitations, the authors emphasized the fact that the method is strongly dependent on the observer, which may result in differences in the FMD determination. This limitation is also related to the accuracy of the diameter measurements of the ultrasonic scan of the artery, and thus directly depends on the axial and elevation resolution of the US system used. The axial resolution of the standard US scanners working at 7–12 MHz, used in the papers cited above, is within the range of 0.2–0.3 mm, which is close to the change of brachial or radial artery diameter and thus resulting in severe biasing the final results.

The aim of our study is to show that the redesigned (in comparison with the system previously described (Nowicki *et al.*, 2018)) high frequency scanning/Doppler probe dedicated to image the radial artery within narrowest part of the elevation beam allows measuring the FMD and SR in the radial artery with higher accuracy than the systems using frequencies below 12 MHz. The efficiency and usefulness of this system were confirmed in a preliminary study of FMD and SR in 26 subjects; 12 normal healthy subjects and 14 patients with stable coronary artery disease.

This paper is organized as follows. In Sec. 2 we describe the experimental setup and our probe, the assembly of L40-8 linear array transducer combined with 20 MHz multigate pulse Doppler. The measurement protocol is also explained in this section. The results of measurements of the axial resolution for two US scanners with carrier frequencies of 6.8 MHz and 16.8 MHz are presented in the next section. The validation of the system is done through measurements of FMD and SR in the radial artery of healthy subjects and patients with stable coronary artery disease. The statistical analysis of the obtained data is also presented in this section. Finally, in two last sections, the discussion and conclusions are presented.

2. Material and methods

2.1. Axial resolution

Firstly, we have compared the axial resolution of two US scanners with L14-5 linear array transducer (6.8 MHz center frequency) and L40-8 linear array transducer (16.8 MHz center frequency), both from Ultrasonix SonixTouch-Analogic Corporation, Peabody, MA, USA. The axial length Δd of the scanning pulse (for echo) is equal to half of the pulse duration $\tau/2$ and is directly proportional to the speed of sound c in the investigated tissue. The shorter the time τ of the scanning pulse, the larger the transducer bandwidth B. Generally, the bandwidth is determined at the frequency span where the amplitude drops down to half (−6 dB) of the maximum amplitude at the carrier frequency, $\tau = 1/B_{-6\,\mathrm{dB}}$. The spatial length of the scanning pulse and transducer bandwidth are then related according to the formula $\Delta d_{-6\,\mathrm{dB}} = c/(B_{-6\,\mathrm{dB}})$. A more conservative axial resolution is directly proportional to the length of the scanning pulse and is equal to half the spatial pulse length (SPL). SPL is the product of the number of cycles in an ultrasound pulse and the wavelength λ (SPL = λ number of cycles in the pulse). The beam pressure field was measured using Needle Hydrophone 0.2 mm (Precision Acoustics, Dorchester, UK).

The effective axial resolutions of two scanning systems (L14-5 linear array probe with mean scanning frequency = 6.8 MHz and L40-8 linear array probe with mean scanning frequency = 16.8 MHz) were experimentally determined by the imaging of closely positioned two plastic foils immersed in water.

The influence of the elevation thickness of these two linear arrays on the precision of vessel diameter estimation was also evaluated by measurements of elevation beam widths and systolic/diastolic radial artery diameters measurements in three normal healthy subjects.

2.2. FMD and SR measurements

The FMD is expressed as a percentage change of the initial (baseline) diameter Db to the post-stimulus maximum diameter Dpeak of the artery and is given by the formula $\mathrm{FMD}\,[\%] = ((D_{\mathrm{peak}} - D_b)/D_b)\cdot 100\%$. The normalization of FMD to a shear rate is done by dividing the peak FMD by the accumulated value of shear rate area under the curve (SRAUC). SRAUC is calculated for the time between releasing of the cuff and the peak dilation. The blood flow velocity was recorded for 150 seconds after releasing the pressure cuff.

We have compared the Doppler sensitivity of pulse Doppler modality in a L40-8 linear array transducer (Ultrasonix SonixTouch-Analogic Corporation, Peabody, MA, USA) and 20 MHz single crystal pulse Doppler. The precision of Doppler velocity recordings in the radial artery directly results in the calculation of the shear rate in this artery both in systolic and diastolic phases.

In the L14-5 linear array transducer, the Doppler mode operates at 6 MHz, which is the lower end of the available bandwidth in this specific transducer. In the L40-8 linear array transducer, the Doppler mode operates at about 10 MHz. The sensitivity of 20 MHz single transducer Doppler modality and Doppler incorporated in L40-8 linear array were compared with *in vivo* experiments in three volunteers.

In the arteries, the blood flow velocity profile differs from the parabola, especially near the branches and

in the stenosis. Roevros (1974) proposed a general expression describing velocity profiles for steady flows

$$v(r) = v_{\max}\left[1 - \left(\frac{r}{R}\right)^n\right], \quad n \geq 1, \tag{1}$$

where n represents the shape of the velocity profile, $v_{\max}$ is the maximum velocity, and R is vessel radius. For $n = 2$, Eq. (1) is the parabolic equation. The larger the n, the more the profile is flattened.

The volumetric flow per unit time Q is expressed as

$$Q = \int_0^R v(r) 2\pi \, \mathrm{d}r = \int_0^R v_{\max}\left[1 - \left(\frac{r}{R}\right)^n\right] 2\pi r \, \mathrm{d}r$$

$$= 2\pi R^2 v_{\max}\left(\frac{n}{n+2}\right). \tag{2}$$

The average velocity (v_{avg}) is calculated by dividing the Q-value by the cross-sectional area of the tube

$$v_{\text{avg}} = \frac{Q}{\pi R^2} = v_{\max}\left(\frac{n}{n+2}\right). \tag{3}$$

After substitution Eq. (3) into Eq. (1), we get the expression on the blood flow velocity profile for different exponents of n:

$$v_z(r) = \frac{v_{\text{avg}}}{\left(\frac{n}{n+2}\right)}\left[1 - \left(\frac{r}{R}\right)^n\right]. \tag{4}$$

The shear rate γ on the vessel wall is

$$\gamma = \frac{\mathrm{d}v}{\mathrm{d}r} = \frac{v_{\text{avg}}(n+2)}{n} n \left(\frac{r^{n-1}}{R^n}\right)\Bigg|_{r=R}$$

$$= \frac{v_{\text{avg}}(n+2)}{R} = \frac{2v_{\text{avg}}(n+2)}{R}, \tag{5}$$

where D is the vessel diameter.

For parabolic profile ($n = 2$), $\gamma = 8v_{\text{avg}}/D$ or $\gamma = 4v_{\max}/D$.

2.3. Experimental setup

An experimental setup consisted of a SonixTouch ultrasound scanner with a L40-8 linear array transducer for imaging only, and additional 1.5 mm diameter, single-element 20-MHz multigate Doppler probe attached to the array dedicated for blood flow velocity profile measurements. The design of the probe has been modified compared to the one described previously in the (Tortoli *et al.*, 2006). The Doppler probe and linear array were placed in a plastic housing filled with water and the front end of the container was sealed using plastic foil. The distance from the linear array transducer face to the foil was set to 5 mm while the Doppler transducer was placed where it was almost touching the plastic foil surface, Fig. 1. The reason for moving the linear head 5 mm above the skin was an attempt to perform a radial artery imaging (running from 3 to 5 mm below the surface of the skin) in the narrowest area of the ultrasound beam in the elevation. The angle between the Doppler beam and the foil surface was 68°. The PRF for linear array and Pulse Doppler are not coherent and a certain beat frequency, resulting from the cross talk of both transmitted signals, interferes in final Doppler. For that reason a cork separator preventing the cross talk in the direct water path was added.

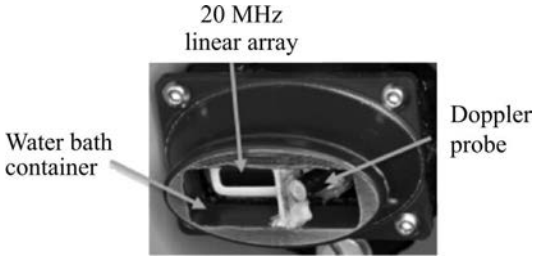

Fig. 1. L40-8 linear array combined with 20 MHz Doppler probe.

The Doppler signal is recorded using the acquisition board and GASP software developed at the University of Florence (Tortoli *et al.*, 2006). The Doppler signal from the center of the blood vessel is selected for further processing. It corresponds to the peak flow velocity. A detailed explanation of the Doppler system and the technique of measuring radial artery diameter and blood flow velocity have previously been described in our paper 15.

2.4. Protocol of FMD and SR measurements in patients

The in vivo validation of the usefulness of the designed system for measurements of FMD and SR in the radial artery, was performed in the study of two groups of patients: Group I consisted of 12 normal healthy subjects, 7 men and 5 women (41–73 yr old); Group II consisted of 14 patients, 12 men and 2 women (40–77 yr old), with invasively confirmed chronic stable coronary artery disease (CAD). All subjects were measured between 11 am and 1 pm after fasting for about 3 hours. The examined CAD patients were stented.

The subjects examined gave their written, informed consent to participate and underwent simultaneous testing with the radial artery reactive response using ultrasound imaging and Doppler signals. The study protocol was approved by the Human Investigation Review Committee at the Military Medical Institute – Warsaw, Poland.

Data processing and statistical analysis were done using the R programming language for statistical computing and graphics (https://www.r-project.org). Continuous variables, FMD and SR were described by statistical characteristics, i.e., the mean and standard de-

viation. The normality of the random variable distributions in groups was verified using the Shapiro-Wilk test. A confidence level of 0.95 was established in all statistical calculations and for all performed statistical tests. The differences between groups were tested by the Kolmogorov-Smirnov (KS) and Mann-Whitney-Wilcoxon (MWW) tests.

3. Results

3.1. Measurements of axial resolution

The scanning pulses for two US systems using the L14-5 (6.4 MHz center frequency) and L40-8 (15.6 MHz center frequency) linear arrays, and the spectra of the pulses reflected from the perfect reflector in water are shown in Fig. 2. The axial resolutions $\Delta d_{-6\,\mathrm{dB}}$ were calculated from recordings of echoes from a perfect reflector, being equal 0.36 mm and 0.14 mm for probes L14-5 and L40-8, respectively, Fig. 2. The SPL/2 values for these two probes equal 0.16 mm and 0.07 mm, respectively.

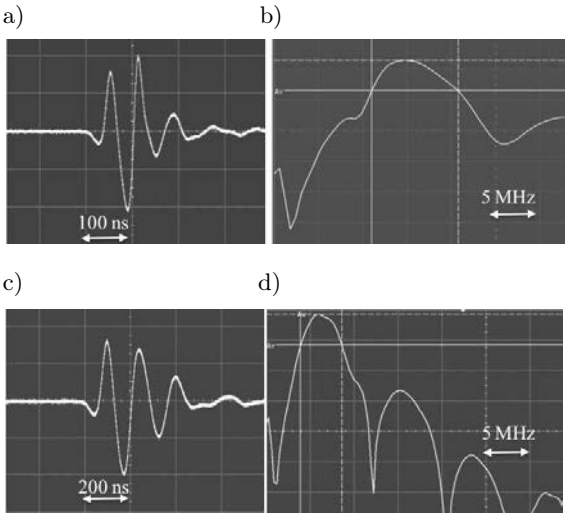

Fig. 2. The length of the ultrasonic pulse depends on the transducer bandwidth (a) the L40-8 linear array (center frequency 16.8 MHz) generates a pulse (−6 dB) duration below 0.1 μs with the bandwidth (−6 dB) of 9.8 MHz (b); (c) the L14-5 linear array (center frequency 6.8 MHz) generates impulses (amplitude −6 dB) lasting 0.32 μs with the bandwidth (−6 dB) of 4.7 MHz (d).

Next, the images of two samples of plastic food wrap foils (0.07 mm thick) placed in front of the scanning transducer were recorded. The spacing between foils was set to 0.4 mm and 0.2 mm. The scans of foils spaced apart by 0.2 mm are shown in Figs 3a and 3b, while images of foils separated by 0.4 mm are shown in Figs 3c and 3d. Scans presented in Figs 3a and 3c were recorded using the 7–12 MHz linear array; scans presented in Figs 3b and 3d were recorded using the 20 MHz linear array.

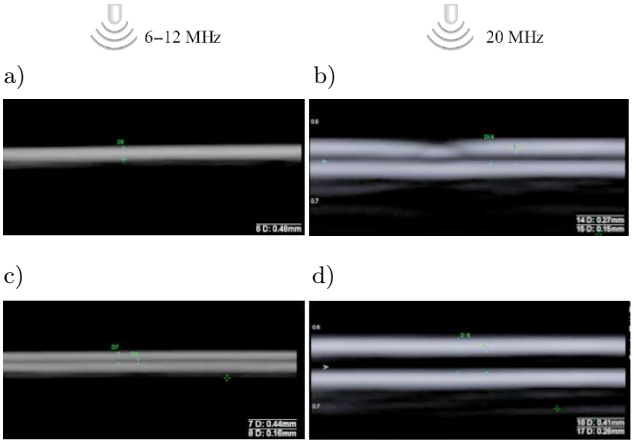

Fig. 3. Images of two samples of plastic food wrap foils (0.07 mm thick) spaced apart by 0.2 mm (a and b) and 0.4 mm (c and d) scanned with L14-5 probe and L40-8 probe, respectively.

The beam widths measured across the elevation plane for both examined linear arrays are shown in Fig. 4. The beam width for the L40-8 probe equals 1.6mm, and is almost twice as narrow as the beam width of the L14-5 probe, which equals 2.5 mm. The latter is close to the average diameter of radial arteries examined in our study group and is the source of artifacts smearing the cross-section image of the vessels.

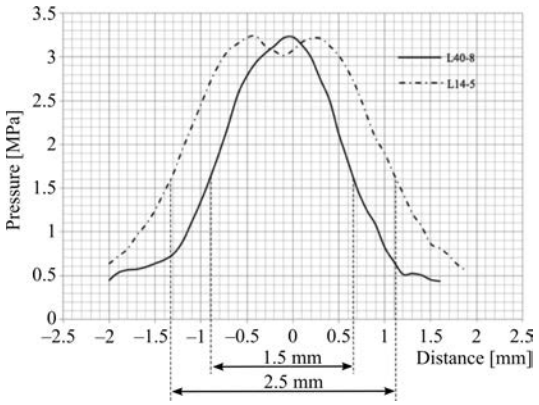

Fig. 4. The plot of the elevation beams width for linear arrays L14-5 (dotted line) and L40-8 (solid line) measured in water 8 mm below the transducer face. FWHMs for both arrays are 2.5 and 1.5 mm, respectively.

3.2. Comparative studies of effective axial resolution in three volunteers

The effective axial resolutions in vessel diameter measurements were carried out in three volunteers (63, 65, and 73 yr old) according to the following protocol. The L14-5 linear array transducer was fixed over the radial artery and the cine-loops sequences of the pulsating artery scans were recorded in AVI format (Audio Video Interleave) for approximately 40 seconds.

The same measurement was then made using the L40-8 linear array transducer. In both cases, the maximum and minimum diameters of the arteries in systole and diastole were determined using Brachial Analyser (BA) software (Medical Imaging Applications, LLC, Coralville, IA) and the average dilatation level was calculated for four consecutive heart cycles (Fig. 5).

The results obtained with the use of the L40-8 probe varied between systole and diastole by 0.1–0.2 mm and the ratio of systolic/diastolic dilation SDD [%] = ((systolic diameter – diastolic diameter)/diastolic diameter)·100% was from 4% to 6% for three examined subjects. Changes observed with the L14-5 probe were very small and recorded at the second place after the decimal point (i.e. below the axial resolution) and the ratio of diameters in contraction and diastole did not exceed 1%.

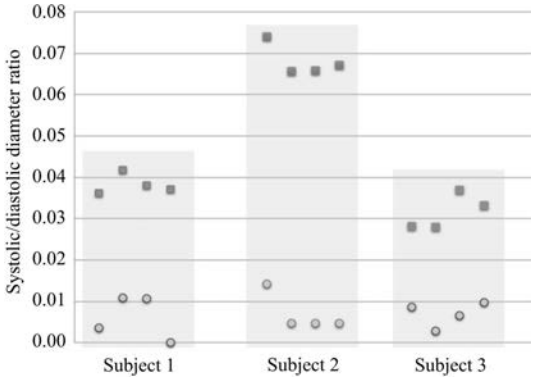

Fig. 5. Comparison of measurements of relative radial artery dilation, SDD = (systolic diameter – diastolic diameter)/diastolic diameter in three volunteers using L40-8 probe (squares symbols) and L14-5 probe (circles symbols) scanning probes, respectively. In all three cases, the calculated average systolic/diastolic dilation for scanning using L14-5 probe never exceeded 1%, while when using L40-8 scanning probe, the difference between the systole and diastole was clear and averaged 4%, 6.5%, and 3.2%, respectively.

3.3. Shear rate measurements

In order to compare the sensitivity of the 10 MHz linear array operated Doppler and the 20 MHz single transducer Doppler, simultaneous recordings of blood flow in the radial arteries of three volunteers were done and signal to noise ratios were calculated. For the 20 MHz pulsed Doppler, the calculated signal-to-noise ratio was 28, 31, and 30 dB for the three subjects, respectively. The Doppler signal recorded using the linear array transducer L40-8 (the actual carrier frequency for Doppler mode equaled 10 MHz) had worse signal-to-noise performance, which equaled 9.9 dB, and 11 dB, respectively for the same examined patients. As the sensitivity of the 20 MHz Doppler system was about 10 times greater than the Doppler incorporated into the linear array, all the Doppler measurements reported in this paper were performed using a single element 20 MHz pulse Doppler combined with a 20 MHz linear array probe, shown in Fig. 1.

The precise measurements of the blood flow velocity profiles were done in the radial arteries in 6 subjects in order to determine the deviation of the actual velocity profiles from the parabolic shape. The best fittings of velocity profile given by Eq. (4) to the measured profiles were obtained for $1.8 < n < 2.4$; therefore for simplicity we assumed $n = 2$ in further calculations. In calculations of SR, D was assumed to be equal to the mean value of the peak vessel diameter measured during the time from cuff release to maximum artery diameter dilation. An exemplary spectrum type velocity profile recording is shown in Fig. 6 where white line represents the mean velocity profile calculated during the systolic phase.

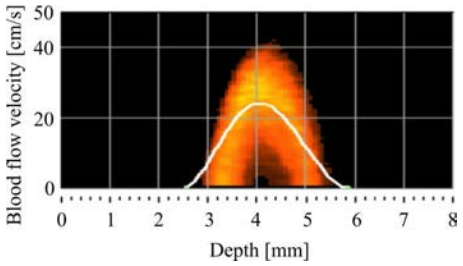

Fig. 6. Typical recording of the spectral profile in the radial artery, where white line represents the mean velocity profile calculated during systolic phase. The best fitting of the mean velocity to the velocity profile given by Eq. (4) is obtained for $n = 2.1$.

3.4. FMD and FMD/SR measurements

In Group I, the FMD was in the range of 7–16% with mean ± sd equal to 11.53 ± 2.72%; the FMD for Group II was in the range 0.1–7 % and mean ± sd equaled 3.01 ± 1.96%. In Group I, the FMD/SR equaled $3.08 \cdot 10^{-4} \pm 1.38 \cdot 10^{-4}$; in Group II, the FMD/SR equaled $0.89 \cdot 10^{-4} \pm 0.64 \cdot 10^{-4}$, respectively.

The FMD variables for both groups and the FMD/SR for Group II were normally distributed. They were confirmed by p-values < 0.05 for the Shapiro-Wilk test; the FMD/SR variables for Group I were not normally distributed and yielded a p-value < 0.05 for the Shapiro-Wilk test. The differences in FMD/SR values between groups were tested only by the non-parametric tests, i.e., Kolmogorov-Smirnov (KS) or Mann-Whitney-Wilcoxon (MWW), while the FMD values were tested by the t-test. All performed tests had p-values < 0.0005. The boxplots graphs for FMD and FMD/SR are presented in Fig. 7.

The utility of group differentiation by FMD and FMD/SR values in diagnostic tests are expressed with ROC (receiver-operator characteristics) curves, which are shown in Fig. 8 together with the values of AUC

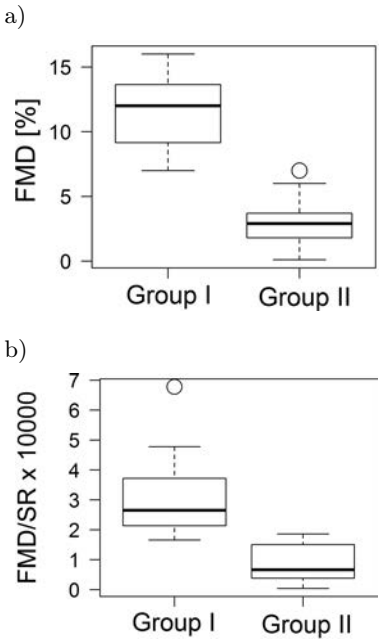

Fig. 7. a) Boxplots of FMD, b) boxplots of FMD/SR; Group I contains normal healthy subjects, and Group II contains patients with CAD (boxplots are classical Tuckey plots, the bold transverse line indicates the median).

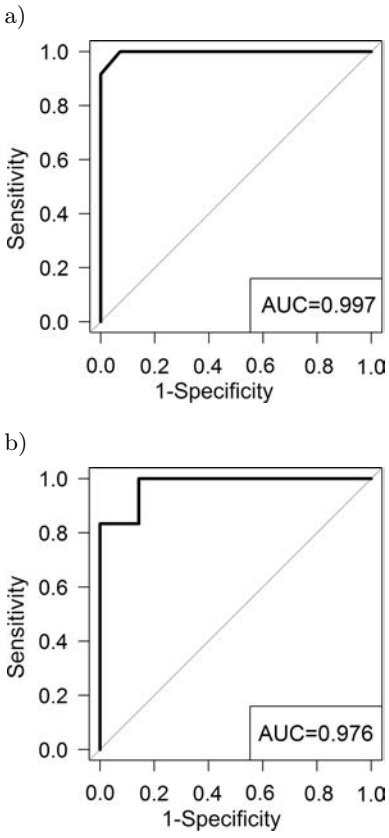

Fig. 8. a) ROC curve for FMD and b) ROC curve for FMD/SR as CAD predictors.

(area under the curve), which equal 0.997 and 0.976 for FMD and FMD/SR predictors, respectively.

4. Discussion

In laboratory tests, the axial resolution and sensitivity of Doppler measurements of the designed US system at 20 MHz and standard ultrasound operated on the 7–12 MHz frequency were compared.

The US images of two plastic foils shown in Fig. 3 proved that the precision in axial resolution is almost three times less for the 7–12 MHz transducer than the one for the 20 MHz probe. The echoes from targets positioned 0.2 mm apart were clearly separated using the 20 MHz probe, while they were indistinguishable when scanned with the 7–12 MHz probe. In the case of imaging foils spaced 0.4 mm apart from each other, the echoes from the upper and the lower foil separated for both probes.

The axial resolution of the high frequency (about 20 MHz) system is approximately 0.1 mm but it should be emphasized that in the case of imaging of rounded structures such as the walls of arteries, the axial resolution is impaired by the finite lateral thickness of the ultrasonic beam in the elevation.

The echoes from the structure are not reflected in the desirable scan plane but contain contributions from the space covered by the ultrasonic beam in the elevation plane and thus result in reduced local contrast. This property of an ultrasound beam transmitted from a linear array is the source of echo blurring, especially from spherical interfaces between tissue structures, e.g. vessel walls. This characteristic feature of ultrasonic scanning often manifests itself in the difficulty of precise estimation of the intima/media thickness, especially on the anterior wall of the artery. Similarly, the thicker the slice in the elevation plane, the more difficult it is to properly assess the dilatation of the vessel (especially the position of the anterior wall during the heart cycle).

The −6 dB beam thickness for the 20 MHz probe equaled 1.7 mm, which was almost twice as narrow as the beam width of the 7 MHz L14-5 probe (Fig. 4).

We have shown the influence of the elevation thickness of the beam on the measurements of small changes in vessel diameter (Fig. 5). SDD changes in the radial artery were practically immeasurable, not exceeding 1% when using the lower frequency probe, while they were clearly seen, from 4% to 7%, when scanning radial artery with the 20 MHz probe.

The signal backscattered on red blood cells roughly increases with the fourth power of the scanning frequency and doubling the transmitted frequency in the Doppler from 10 MHz to 20 MHz results in a significant increase of the signal-to-noise ratio. In terms of Doppler measurements it means more accurate measurement of blood flow velocity, and subsequently a more accurate calculation of the shear rate.

The measured sensitivity of the external 20 MHz pulse Doppler system was about 10 times greater than

the Doppler in the L40-8 linear array transducer. It provides a more precise measurement of blood flow velocity, especially low velocities during diastole, resulting in a more accurate determination of the shear rate.

Due to the range of the systolic blood flow velocity in the radial artery measured in all examined subjects, the blood was assumed to behave as a Newtonian fluid with a constant viscosity coefficient. Considering a linear relationship between the shear stress and the rate of strain, the shear stress variations had been included as the strain rate variations. Moreover, the blood flow exhibited velocity profiles that were very close to parabolic curves. This assumption simplified the calculations of SR values.

The value of the high frequency system was validated in vivo measurements of FMD and SR in the radial arteries of 12 normal healthy subjects and 14 CAD patients. Statistical analysis showed that FMD and FMD/SR exhibited a significant univariate association with the occurrence of CAD, confirmed by the p-value for the MMW test. The results revealed that the range of FMD obtained in normal healthy subjects did not coincide with the range of FMD measured for CAD patients. The normalized FMD/SR had a range of values for healthy subjects and for patients but it lied in the first FMD quartile and in the fourth FMD/SR quartile, which indicated evident differences between the groups. The analysis of the ROC curve (Fig. 8) for the prediction of CAD patients based on FMD values showed that the value of 7% could be used as a cut-off level to predict CAD patients with a sensitivity of 100% and a specificity of 92.9%. The same analysis performed for the ROC curve for the prediction of CAD patients based on FMD/SR values showed that a value of $1.86 \cdot 10^{-4}$ could be used as a cut-off to predict CAD patients with a sensitivity of 100% and a specificity of 85.76%. We note that FMD/SR had a slightly lower AUC value than FMD alone.

5. Conclusions

According to laboratory phantom experiments and in vivo measurements in radial artery of three normal healthy subjects, we showed the advantage of using high-frequency ultrasound (20 MHz). It provides greater resolution and a more sensitive Doppler over a standard 7–12 MHz scanning system resulting in a more accurate estimation of artery diameter and a blood flow velocity. This means that using the 20 MHz scanning system and the external pulse 20 MHz Doppler ultrasound leads to more reliable measurements of both the blood flow and the dilation of the radial artery than using standard US with Doppler directly transmitted from a linear array.

The statistical analysis of the results for both groups of subjects, normal healthy subjects and CAD patients, showed the diagnostic predictive strength of FMD and FMD/SR based on the p-values of relevant tests and the ROC analysis with very high AUC values. However, the number of subjects was rather small and it is evident that in order to improve the diagnostic value of the obtained results, it is necessary to conduct the research on a larger population.

This introductory analysis confirmed the effectiveness of the 20/20 MHz system for the measurements of radial artery dilation and blood flow in the exemplary study of identifying CAD predictors.

Conflicts of interest

None.

Acknowledgments

This work was supported by National Science Center, Grant Number UMO-2017/25/B/ST7/01601.

References

1. Cahill P.A., Redmond E.M. (2016), *Vascular endothelium – Gatekeeper of vessel health*, Atherosclerosis, **248**: 97–109, doi: 10.1016/j.atherosclerosis.2016.03.007.
2. Celermajer D.S. *et al.* (1992), *Non-invasive detection of endothelial dysfunction in children and adults at risk of atherosclerosis*, Lancet, **340**(8828): 1111–1115, doi: 10.1016/0140-6736(92)93147-F.
3. Deanfield J.E., Halcox J.P., Rabelink T.J. (2007), *Endothelial function and dysfunction: testing and clinical relevance*, Circulation, **115**(10): 1285–1295, doi: 10.1161/CIRCULATIONAHA.106.652859.
4. Deshko M.S., Snezhitsky V.A., Dolgoshey T.S., Madekina G.A., Stempen T.P. (2011), *Flow-mediated dilation in patients with paroxysmal atrial fibrillation: initial evaluation, treatment results, pathophysiological correlates*, Europace, **13** (supplement 3), https://insights.ovid.com/ep-europace/europ/2011/06/003/flow-mediated-dilation-patients-paroxysmal-atrial/644/00127069.
5. Gutiérrez E., Flammer, A.J., Lerman, L.O., Elízaga, J., Lerman, A., Fernández-Avilés F. (2013), *Endothelial dysfunction over the course of coronary artery disease*, European Heart Journal, **34**(41): 3175–3181, doi: 10.1093/eurheartj/eht351.
6. Harris R.A., Nishiyama S.K., Wray D.W., Richardson R.S. (2010), *Ultrasound assessment of flow-mediated dilation*, Hypertension, **55**(5): 1075–1085, doi: 10.1161/HYPERTENSIONAHA.110.150821.
7. Koeth R.A., Haselden V., Wilson Tang W.H. (2013), *Chapter one – myeloperoxidase in cardiovascular disease*, Advances in Clinical Chemistry, **62**: 1–32, doi: 10.1016/B978-0-12-800096-0.00001-9.

8. Lehoux S., Jones E.A. (2016), *Shear stress, arterial identity and atherosclerosis*, Thrombosis and haemostasis, **115**(3): 467–73, doi: 10.1160/TH15-10-0791.

9. Nowicki A. *et al.* (2018), *20-MHz ultrasound for measurements of flow-mediated dilation and shear rate in the radial artery*, Ultrasound in Medicine & Biology, **44**(6): 1187–1197, doi: 10.1016/j.ultrasmedbio.2018.02.011.

10. Padilla J. *et al.* (2008), *Normalization of flow-mediated dilation to shear stress area under the curve eliminates the impact of variable hyperemic stimulus*, Cardiovascular Ultrasound, **6**(1): 44, doi: 10.1186/1476-7120-6-44.

11. Pyke K.E., Dwyer E.M., Tschakovsky M.E. (2004), *Impact of controlling shear rate on flow-mediated dilation responses in the brachial artery of humans*, Journal of Applied Physiology, **97**(2):499–508, doi: 10.1152/japplphysiol.01245.2003.

12. Pyke K.E., Tschakovsky M.E. (2007), *Peak vs. total reactive hyperemia: which determines the magnitude of flow-mediated dilation*, Journal of Applied Physiology, **102**(4): 1510–1519, doi: 10.1152/japplphysiol.01024.2006.

13. Roevros J.M.J.G. (1974), *Analogue processing of C.W. flowmeter signals to determine average frequency shift momentaneously without the use of a wave analyser*, [in:] Reneman R.S. [Ed.], *Cardiovascular applications of ultrasound*, pp. 43–54, Amsterdam: North-Holland.

14. Storch A.S., de Mattos J.D., Alves R., dos Santos Galdino I., Rocha H.N.M. (2017), *Methods of endothelial function assessment: description and applications*, International Journal of Cardiovascular Sciences, **30**(3): 262–273, doi: 10.5935/2359-4802.20170034.

15. Tortoli P., Morganti T., Bambi G., Palombo C., Ramnarine K.V. (2006), *Noninvasive simultaneous assessment of wall shear rate and wall distension in carotid arteries*, Ultrasound in Medicine & Biology, **32**(11): 1661–1670, doi: 10.1016/j.ultrasmedbio.2006.07.023.

16. Yousuf O. *et al.* (2013), *High-sensitivity C-reactive protein and cardiovascular disease: a resolute belief or an elusive link?*, Journal of the American College of Cardiology, **62**(5): 397–408, doi: 10.1016/j.jacc.2013.05.016.